

# Supplemental Material

## I. CLOCK MEASUREMENT SEQUENCE

**State Detection:** The signal for each interrogation are the 468 nm photons spontaneously emitted by the radium ion, which are collected onto a photomultiplier tube (PMT), Hamamatsu H10682-210. During 0.5 ms of state detection 25 photons are collected on average if the population is in the  $S_{1/2}$  or  $D_{3/2}$  states, and 1.5 photons of background scattered light are collected if the population is shelved in the  $D_{5/2}$  clock state. We set the bright-state detection threshold to 5.5 counts.

**State Preparation:** We simultaneously drive the  $|S_{1/2}, m = \mp 1/2\rangle \rightarrow |D_{5/2}, m = \pm 3/2\rangle$ ,  $D_{3/2} \rightarrow P_{1/2}$ , and  $D_{5/2} \rightarrow P_{3/2}$  transitions to prepare the population in the  $|S_{1/2}, m = \pm 1/2\rangle$  state.

**Cleanout:** To prepare for the next interrogation any population shelved in the clock state is cleaned out with light at 802 nm, where decays from the  $P_{3/2}$  state populate the  $S_{1/2}$  and  $D_{3/2}$  states.

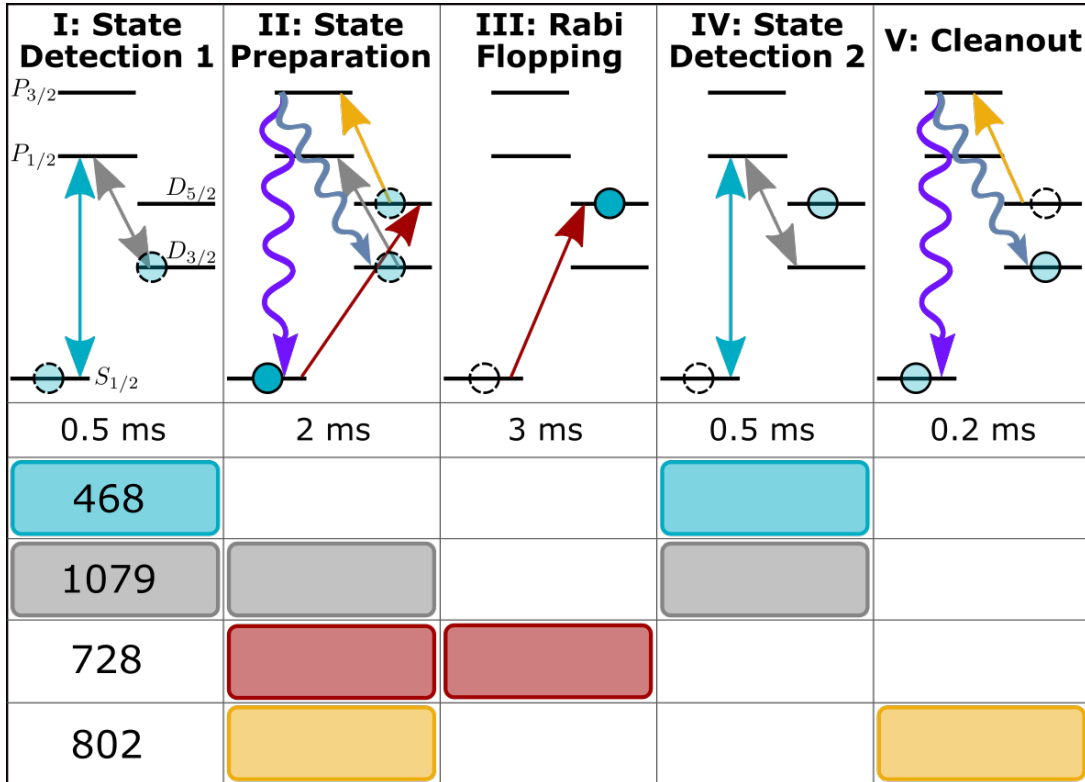


FIG. S1. The measurement sequence for a single interrogation. There is a 5 ms Doppler cool period after the first state detection which is not shown in the figure. Squiggly lines depict E1 allowed decays, straight lines show optical pumping transitions, and double-arrows indicate optical cycling transitions.

## II. LOCK SERVO

The individual locking servos update the frequency detuning of each Zeeman transitions by  $\Delta\nu$ , following,

$$\Delta\nu = GE + r_{\text{cavity}}t_c, \quad (\text{S1})$$

where  $E = (n_b - n_r)/n$  is the error signal defined in the text,  $G$  is a gain parameter,  $t_c$  is the total interrogation cycle time (10 s),  $r_{\text{cavity}}$  is the cavity drift rate ( $\sim 0.2$  Hz/s). The cavity drift rate is updated with the average frequency of all transitions probed using an integral servo, with a time constant of  $\sim 1000$  s.

### III. CLOCK SYSTEMATICS

#### A. Excess micromotion shifts

##### 1. Second-order Doppler shift

The second-order Doppler shift in fractional form is

$$\frac{\Delta\nu_{\text{D2}}}{\nu_0} = - \left( \frac{\Omega}{\omega_0} \right)^2 \sum_{x,y,z} R_i, \quad (\text{S2})$$

where  $\nu_0$  is the radium clock transition frequency in Hz,  $\Omega$  is the trap rf drive frequency,  $\omega_0 = 2\pi\nu_0$ , and  $\sum R_i$  is the sum of the micromotion sideband intensity ratios [? ]. We use  $\nu_0 = 412\,007.701(18)$  GHz [? ],  $\Omega_{\text{rf}}/2\pi = 993$  kHz, and  $\sum R_i = 0.74(8)$ , which we determine from measuring the micromotion sidebands in three near-orthogonal directions. We calculate  $\Delta\nu_{\text{D2}} = -1.77(19)$  mHz.

##### 2. Scalar Stark shift

The scalar Stark shift in fractional form is

$$\frac{\Delta\nu_{\text{scalar}}}{\nu_0} = - \frac{\Delta\alpha_0}{\hbar\omega_0} \left( \frac{m\Omega^2 c}{e\omega_0} \right)^2 \sum_{x,y,z} R_i, \quad (\text{S3})$$

where  $\Delta\alpha_0$  is the differential static scalar polarizability and  $m$  is the mass of the ion [? ]. We use  $\Delta\alpha_0 = -22.2(1.7)$  a.u. [? ]. We calculate  $\Delta\nu_{\text{scalar}} = 0.045(6)$  mHz.

##### 3. Tensor Stark shift

The maximum possible tensor stark shift in fractional form is

$$\frac{\Delta\nu_{\text{tensor}}}{\nu_0} = - \frac{\alpha_2}{\hbar\omega_0} \left( \frac{m\Omega^2 c}{e\omega_0} \right)^2 \sum_{x,y,z} R_i, \quad (\text{S4})$$

where  $\alpha_2$  is the  $D_{5/2}$  state tensor polarizability [? ]. We use  $\alpha_2(D_{5/2}) = -52.6(5)$  a.u. [? ]. We calculate  $\Delta\nu_{\text{tensor}} = 0.108(12)$  mHz. We use the sum of the maximum shift and uncertainty, 0.120 mHz, as the uncertainty for this shift.

## B. Thermal motion shift

### 1. Second-order Doppler shift

The fractional second-order Doppler shift due to the ion's secular motion is

$$\frac{\Delta\nu_{D2}}{\nu_0} = -\frac{5kT_{\text{ion}}}{2mc^2}, \quad (\text{S5})$$

where  $T_{\text{ion}}$  is the temperature of the ion, and  $k$  is Boltzmann's constant [? ? ?]. We measured the ion temperature along in the axial and radial mode directions by driving Rabi oscillations on the clock transition and determined an average temperature of  $T_{\text{ion}} = 0.6$  mK. We estimate the temperature uncertainty to be 0.6 mK to account for fluctuations in Doppler cooling laser frequencies and any temperature imbalance between different secular motion modes. This measured  $T_{\text{ion}}$  is consistent with the Doppler cooling limit  $T_c = 0.4$  mK. The corresponding frequency shift is  $\Delta\nu_{D2} = -0.3(3)$  mHz.

### 2. Scalar Stark shift

The fractional scalar Stark shift due to the ion's thermal motion is

$$\frac{\Delta\nu_{\text{scalar}}}{\nu_0} = -\frac{kT_{\text{ion}}}{mc^2} \frac{\Delta\alpha_0}{\hbar\omega_0} \left(\frac{m\Omega c}{e}\right)^2, \quad (\text{S6})$$

where  $T_{\text{ion}}$  is the temperature of the ion [? ? ?]. Here, the shift is measured to be  $\Delta\nu_{\text{scalar}} = 0.003(3)$  mHz.

## C. Electric quadrupole shift

The electric quadrupole shift is cancelled because we are averaging Zeeman pairs. We can approximate the uncertainty on this cancellation from the electric quadrupole shift magnitude,  $A_Q = [\Delta f_Q(m_{j'} = 5/2) - \Delta f_Q(m_{j'} = 1/2)]/6$  [?]. From the frequency difference between shifted pairs we determine the average drift rate of  $A_Q$  to be  $-1.3$   $\mu\text{Hz/s}$ . Given our cycle time of 10 s we estimate the electric quadrupole shift uncertainty to be 0.013 mHz.

## D. Clock laser ac Stark shift

**728 nm:** The ac Stark shift due to off-resonant dipole coupling is

$$\Delta\nu_{\text{ac}}(\lambda) = -\frac{\Delta\alpha_{\text{ac}}(\lambda)}{2hc\epsilon_0} I = \kappa(\lambda)I, \quad (\text{S7})$$

where  $\Delta\alpha_{\text{ac}}(\lambda) = \Delta\alpha_{\text{ac}}(D_{5/2}, \lambda) - \Delta\alpha_{\text{ac}}(S_{1/2}, \lambda)$ ,  $\lambda$  is the laser wavelength and  $\kappa(\lambda)$  is the ac Stark shift intensity coefficient [?]. Using  $\Delta\alpha_{\text{ac}}(D_{5/2}, 728 \text{ nm}) = -169(4)$  a.u. and  $\Delta\alpha_{\text{ac}}(S_{1/2}, 728 \text{ nm}) = 140(3)$  a.u. [?], we calculate  $\kappa(728 \text{ nm}) = 1.45(2)$  mHz/(W/m<sup>2</sup>). We measure the clock laser intensity to be 500(300) W/m<sup>2</sup>. The large uncertainty in the clock laser intensity is due to probing all Zeeman transitions with equal contrast, which requires different AOM driving amplitudes. We calculate the clock laser ac Stark shift to be 0.7(4) Hz.

### E. Quadratic Zeeman shift

The quadratic Zeeman shift is caused by the mixing of the  $D_{5/2}$  and  $D_{3/2}$  sublevels when the ion is exposed to a magnetic field. This shift is

$$\nu_{ZQ} = \langle \nu'_{ZQ}(m_j) \rangle = \frac{2}{15} \left( \frac{[\mu_B B (g_S - 1)]^2}{h^2 \nu_{DD}} \right), \quad (\text{S8})$$

where  $B$  is the magnetic field,  $g_S = -g_e$ ,  $\mu_B$  is the Bohr magneton, and  $\nu_{DD}$  is the energy separation between the  $D_{5/2}$  and  $D_{3/2}$  states [? ]. We use a static magnetic field of  $B = 0.00057369(8)$  T, and  $\nu_{DD} = 49.730\,02(5)$  THz [? ]. We calculate  $\nu_{ZQ} = 173.66(5)$  mHz.

### IV. EVALUATION OF THE LANDÉ G-FACTOR RATIO

From the clock measurement data we calculate three Landé  $g$ -factor ratios from the three Zeeman pairs (C1, C2, and C3) defined in the text. For a given Zeeman transition the frequency detuning from the 728 nm transition center is given by

$$\delta = \kappa \frac{g_D}{g_S} m_D - \kappa m_S, \quad (\text{S9})$$

where  $\kappa = g_S \mu_B B / h$ , and  $g_S$  is the ground state Landé  $g$ -factor,  $\mu_B$  is the Bohr magneton,  $B$  is the magnetic field, and  $h$  is the Planck constant. The C1, C2, and C3 frequency detunings can be written as

$$\begin{aligned} \text{C1} &= \delta_{1/2 \rightarrow 1/2} - \delta_{-1/2 \rightarrow -1/2} = \kappa \left( \frac{g_D}{g_S} - 1 \right) \\ \text{C2} &= \delta_{1/2 \rightarrow 3/2} - \delta_{-1/2 \rightarrow -3/2} = \kappa \left( 3 \frac{g_D}{g_S} - 1 \right) \\ \text{C3} &= \delta_{1/2 \rightarrow 5/2} - \delta_{-1/2 \rightarrow -5/2} = \kappa \left( 5 \frac{g_D}{g_S} - 1 \right) \end{aligned}$$

The frequency ratios of C1, C2, and C3 then directly give three Landé  $g$ -factor ratios

$$\frac{g_D}{g_S} = \frac{\frac{C1}{C3} - 1}{5 \frac{C1}{C3} - 1} = \frac{\frac{C1}{C2} - 1}{3 \frac{C1}{C2} - 1} = \frac{\frac{C2}{C3} - 1}{5 \frac{C2}{C3} - 3} \quad (\text{S10})$$

This method cancels out the electric quadrupole shift as C1, C2, and C3 are the frequency differences between symmetric Zeeman transitions.

### V. AUTLER TOWNES SHIFT

When the energy splitting between the ground state Zeeman sublevels,  $\omega_S = g_S \mu_B B_0 / \hbar$ , equals the rf trapping frequency,  $\Omega_{\text{rf}} / 2\pi = 993$  kHz, there is an Autler-Townes splitting ( $g_S \mu_B B_{\text{trap}} / 2\hbar$ ) of the clock transition due to the trap's magnetic field,  $B_{\text{trap}}$ , driving the  $|S_{1/2}, m = \pm 1/2\rangle \rightarrow |S_{1/2}, m = \mp 1/2\rangle$  transition. To bound  $B_{\text{trap}}$ , we set  $\Omega_{\text{rf}} = \omega_S$  within 1 kHz by changing the static magnetic field  $B_0$ . We did not observe any splitting at the sub 200 Hz

level during direct spectroscopy of individual Zeeman transitions, which indicates that the Rabi frequency due to the trap's magnetic field is not larger than  $\sim 1$  kHz. Therefore the corresponding  $B_{\text{trap}}$  must be no larger than  $7 \times 10^{-8}$  T. The  $B_{\text{trap}}$  shifts the Landé  $g$ -factor ratio,  $g_D/g_S$ , by

$$\frac{g_D}{g_S} = \left[ \frac{1 + \frac{1}{2} \frac{\omega_D^2}{\omega_D^2 - \Omega_{\text{rf}}^2} \frac{\langle B_{\text{trap}}^2 \rangle}{B_0^2}}{1 + \frac{1}{2} \frac{\omega_S^2}{\omega_S^2 - \Omega_{\text{rf}}^2} \frac{\langle B_{\text{trap}}^2 \rangle}{B_0^2}} \right] r, \quad (\text{S11})$$

where  $\omega_D = g_D \mu_B B_0 / \hbar$  and  $r$  is the measured Landé  $g$ -factor ratio at the given static magnetic field [? ]. The shift in the measured Landé  $g$ -factor ratio due to  $B_{\text{trap}}$  is much smaller than the statistical uncertainty of the measured Landé  $g$ -factor ratio.